Structure of rotating charged boson stars

Lucas G. Collodel,* Burkhard Kleihaus, and Jutta Kunz
Institut für Physik, Universität Oldenburg, Postfach 2503 D-26111 Oldenburg, Germany

(Received 11 February 2019; published 29 May 2019)

In this work we present sets of solutions for rotating charged boson stars with different coupling values. By adopting local comoving coordinates, we are able to find expressions for the effective hydrodynamic quantities of the fluids as seen by this class of observers. We show that not only is the energy density nonzero at the center, for the uncharged case it has a local maximum at the core from which it decreases until the point of local minimum where its variation is discontinuous. For the first time (to our knowledge), it is reported how rotating boson stars, charged and uncharged, are completely anisotropic fluids featuring three different pressures. Furthermore, the character of the electromagnetic fields is analyzed.

DOI: 10.1103/PhysRevD.99.104076

I. INTRODUCTION

Gravitationally bound complex scalar fields minimally coupled to gravity, now coined boson stars, have been first realized half a century ago [1,2]. One year later, it was shown that quantized real scalar fields give rise to the same equations of motion when treated semiclassically [3]. The gauged generalizations of boson stars, based on the theory with a local $U(1)$ symmetry, came to be known circa twenty years thereof [4]. The more delicate case of rotating stars was found in the 1990s [5,6] by solving the set of fully nonlinear partial differential equations after a perturbative approach for slow rotation [7] turned fruitless. Thereafter, boson stars became the subject of extensive studies of gravitational physics in the strong regime.

The initial setup of a free massive scalar field gave way to systems with interacting potentials that rendered more massive and astrophysically relevant stars, like the repulsive quartic interaction [8] and the sixtic potential [9] for which solutions were named solitonic stars, for they would exist even in Minkowski spacetime as a self-binding soliton called Q-Ball [10,11]. The solitonic boson star has later been shown to give an appropriate description of what an axion star could be [12].

Rotating boson stars are extremely interesting for their unique properties which highly distinguish them from the more commonly investigated astrophysical objects such as black holes and neutron stars. For instance, their angular momentum is quantized [6], $J = \hbar m N$, where m is a rotation integer and N the particle number. Their family of solutions, stability analysis, existence in higher dimensions, and excited states are reported in [13–21]. Moreover, the topology of the scalar field changes upon rotation as it is then distributed along a torus as required by regularity. As a result, the maximum of their energy density happens off center warping spacetime in an unusual way, and the dynamics of particles freely falling in their spacetime takes a very peculiar form [22,23]. It has recently been shown [24] that when the g_{tt} component of the metric contains a local maximum, which occurs in the surroundings of rotating boson stars, a ring of points is formed where particles initially at rest remain at rest due to an exclusive inertial phenomenon.

In what concerns charged boson stars, their stability, quasibound states around black holes, behavior when critically charged and analytical approximations have broadly appeared in the literature [25–29]. Likewise, the case of charged compact bosons stars, where the scalar field vanishes outside a finite region, has received considerable attention [30–34]. However, the general case when both rotation and charge are present has been less investigated. The system in absence of gravity is discussed in [35], while some properties of rotating charged boson stars in an asymptotically flat spacetime are described in [36], and in four dimensional anti de-Sitter spacetime in [37]. The existence of solutions for hairy Kerr-Newman black holes has also been reported and analyzed in [38].

In this paper we revisit the general case of charged rotating boson stars and construct sets of solutions for different charges and rotation number. A new approach in terms of the hydrodynamic quantities of the fluids is given in local comoving coordinates, so that one can appreciate unambiguously how a certain class of observers measures the energy density and different pressures of the star and how they relate to each other.

The paper is organized as follows. In Sec. II we present the model that describes our system, obtain the partial differential equations and provide the necessary boundary conditions required for solving it and give the expressions for the conserved quantities that arise from the solutions.

*lucas.gardai.collodel@uni-oldenburg.de

The numerical setup is briefly described in Sec. III, where we give the results for the observables for the different parameter sets we solved for. We move to local coordinates in Sec. IV in order to define the energy density and pressures of our fluids, which are then calculated for a selected number of solutions. In Sec. V, the invariants of the electromagnetic field are presented, in comparison to those of a Kerr-Newman black hole. For illustration purposes, we move to local zero angular momentum frames and calculate the components of the electric and magnetic fields. Our conclusions are drawn in Sec. VI. The metric signature is taken to be $(-,+,+,+)$, Greek indices represent coordinate indices, while Latin indices are used for the *vierbein* basis. We use geometrical units such that $c = \hbar = 8\pi G = 1$.

II. THEORETICAL SETTING

In this section the action for charged boson stars and the corresponding Einstein and field equations are presented. The Ansätze for the metric, the boson field, and the electromagnetic potential are given and the boundary conditions for regular, asymptotically flat solutions are considered. Also, the conserved charges and their interrelations are discussed.

A. Action

The system is described by a complex gauged scalar field minimally coupled to gravity,

$$S = \int \left\{ \frac{R}{2} - \frac{1}{2} g^{\mu\nu} [(D_\mu \Phi)(D_\nu \Phi)^* + (D_\mu \Phi)^* (D_\nu \Phi)] - U(|\Phi|) - \frac{1}{4} F^{\mu\nu} F_{\mu\nu} \right\} \sqrt{-\mathfrak{g}} d^4 x, \tag{1}$$

where R is the curvature scalar, Φ is the complex scalar field, U is the self-interaction potential of the scalar field, $F_{\mu\nu} = \partial_\mu A_\nu - \partial_\nu A_\mu$ is the electromagnetic field tensor and $D_\mu \equiv \nabla_\mu + iqA_\mu$ is the covariant derivative that minimally couples the scalar field to the gauge potential A_μ endowing the system with U(1) local symmetry.

Variation of the action with respect to $g^{\mu\nu}$ leads to the Einstein's field equations,

$$G_{\mu\nu} \equiv R_{\mu\nu} - \frac{1}{2} R g_{\mu\nu} = T_{\mu\nu}, \tag{2}$$

where the energy momentum tensor reads

$$T_{\mu\nu} = -g_{\mu\nu} \left\{ \frac{1}{2} g^{\sigma\lambda} [(D_\sigma \Phi)(D_\lambda \Phi)^* + (D_\sigma \Phi)^* (D_\lambda \Phi)] + U(|\Phi|) + \frac{1}{4} F^{\sigma\lambda} F_{\sigma\lambda} \right\} + [(D_\mu \Phi)^* (D_\nu \Phi) + (D_\mu \Phi)(D_\nu \Phi)^*] + F_{\mu\sigma} F_{\nu\lambda} g^{\sigma\lambda}. \tag{3}$$

The field equations of the scalar field are obtained by variation of the Lagrangian with respect to Φ^*

$$D^\mu D_\mu \Phi = \frac{\partial U}{\partial |\Phi|^2} \Phi, \tag{4}$$

and variation of the Lagrangian with respect to the gauge potential yields the Maxwell equations

$$\nabla_\nu F^{\nu\mu} = q j^\mu \tag{5}$$

with conserved electromagnetic current

$$j^\mu = -i(\Phi^* \partial^\mu \Phi - \Phi \partial^\mu \Phi^*) + 2q|\Phi|^2 A^\mu, \quad \nabla_\mu j^\mu = 0. \tag{6}$$

B. Ansätze

We are interested in stationary axisymmetric boson star solutions. We adopt the quasi-isotropic Lewis-Papapetrou metric in adapted spherical coordinates (t, r, θ, φ), for which the line element reads

$$ds^2 = -f dt^2 + \frac{l}{f} \left[g(dr^2 + r^2 d\theta^2) + r^2 \sin^2\theta \left(d\varphi - \frac{\omega}{r} dt \right)^2 \right], \tag{7}$$

where metric functions f, l, g, and ω are functions of r and θ only. This spacetime then possesses two Killing vector fields, namely $\xi = \partial_t$, and $\eta = \partial_\varphi$. In this spacetime, the only off diagonal nonzero components of Einstein's tensor are $G_{t\varphi}$ and $G_{r\theta}$ (and their symmetric counterparts), from which it follows that the gauge potential has only two nontrivial contributions, $A = V(r,\theta) dt + C(r,\theta) d\varphi$. The usual Ansatz for the boson field [6]

$$\Phi(t, r, \theta, \varphi) = \phi(r, \theta) e^{i\omega_s t + im\varphi}, \tag{8}$$

fixes the gauge. Here the boson frequency ω_s and the winding number m are real constants and furthermore m is an integer due to the identification $\Phi(\varphi) = \Phi(\varphi + 2\pi)$. One could instead work with a real scalar field, and the parameters ω_s and m would then appear in the boundary conditions for A_μ. On the other hand, there is no single valued function $h(x^\mu) = \int A_\mu dx^\mu$ for which the gauge transformation $\Phi \to \Phi e^{ih(x^\mu)}$, $A_\mu \to A_\mu - \frac{i}{q} \partial_\mu h(x^\mu)$ makes A_μ trivial everywhere for $F_{\mu\nu} \neq 0$. It is worth noticing that there is a screening mechanism in this system due to the $\phi^2 A_\mu A^\mu$ term in the Lagrangian, which corresponds to a position dependent mass term.

In the absence of gravity, this is the simplest interacting gauge theory one can write down. Indeed, if one is interested in Q-balls, which are bound through their self-interaction, one must adopt nonrenormalizable potentials

[10,39,40]. It was pointed out in [12], based on the pioneering work [3], that real quantized scalar fields yield the same equations of motion as those of complex scalar fields in an entirely classical approach. In this sense, the axion when described by a real quantized scalar field would not give rise to the oscillatons [41] when coupled to gravity, which are time dependent solutions of a gravitationally bound real scalar field obtained through the classical approach. Instead, axion stars are realized by solitonic boson stars. The axion potential is given by

$$U_a(\Phi) = m_a f_a \left[1 - \cos\left(\frac{\Phi}{f_a}\right)\right], \tag{9}$$

where m_a is the axion mass and f_a is the decay constant. In the semiclassical approach, the field is quantized, $\Phi \to \hat{\Phi} = \hat{\Phi}^+ + \hat{\Phi}^-$, and in order to appreciate the action of the potential on the different states and calculate the expectation value of energy-momentum tensor $\langle T^{\mu}{}_{\nu}\rangle$, the self-interaction potential is Taylor expanded,

$$U_a(\Phi) \sim \frac{m_a^2}{2}\Phi^2 - \frac{1}{4!}\frac{m_a^2}{f_a^2}\Phi^4 + \frac{1}{6!}\frac{m_a^2}{f_a^4}\Phi^6 - \cdots. \tag{10}$$

It is shown in [12] that the solutions do not depend strongly on the number of terms considered in the above expansion, as long as the quartic term is present with the correct minus sign. Because we are interested in a theory with a lower bound for the energy, we consider yet the next term in the expansion above adopting the sixtic potential, which also gives rise to Q-balls in the absence of gravity,

$$U(|\Phi|) = \phi^2(m_b^2 - a\phi^2 + b\phi^4), \tag{11}$$

with $m_b^2 = 1.1$, $a = 2$, and $b = 1$. We will keep the boson frequency ω_s, the gauge coupling parameter q, and the winding number m as free parameters, which determine the charged rotating boson star solutions.

C. Boundary conditions

When the Ansätze for the metric, the scalar field, and the gauge field are substituted in Eqs. (2), (4), and (5) the general field equations reduce to a system of coupled nonlinear partial differential equations in r and θ. In order to find asymptotically flat and regular solutions boundary conditions need to be imposed on the functions, respectively their normal derivatives, at the origin and in the asymptotic region, as well as along the symmetry axis. Also, for solutions with even parity boundary conditions in the equatorial plane are imposed.

At the origin, regularity requires that

$$\begin{aligned} &\partial_r f|_{r=0} = 0, \quad \partial_r l|_{r=0} = 0, \quad g|_{r=0} = 1, \quad \omega|_{r=0} = 0, \\ &\phi|_{r=0} = 0, \quad \partial_r V|_{r=0} = 0, \quad C|_{r=0} = 0. \end{aligned} \tag{12}$$

Since our spacetime is asymptotically Minkowski, we need the scalar and electromagnetic fields to be zero at spatial infinity,

$$\begin{aligned} &f|_{r\to\infty} = 1, \quad l|_{r\to\infty} = 1, \quad g|_{r\to\infty} = 1, \quad \omega|_{r\to\infty} = 0, \\ &\phi|_{r\to\infty} = 0, \quad V|_{r\to\infty} = 0, \quad C|_{r\to\infty} = 0, \end{aligned} \tag{13}$$

where we stress again that the values of V and C are set by the gauge.

On the symmetry axis, the elementary flatness conditions sets $g|_{\theta=0} = 1$. The other fields are, once again, determined as to guarantee regularity,

$$\begin{aligned} &\partial_\theta f|_{\theta=0} = 0, \quad \partial_\theta l|_{\theta=0} = 0, \quad g|_{\theta=0} = 1, \quad \partial_\theta \omega|_{\theta=0} = 0, \\ &\phi|_{\theta=0} = 0, \quad \partial_\theta V|_{\theta=0} = 0, \quad C|_{\theta=0} = 0, \end{aligned} \tag{14}$$

and one can appreciate how rotation brings the nontrivial scalar field to possess nontrivial topology.

Finally, because we are describing a system with even parity, all angular derivatives must vanish on the equatorial plane,

$$\begin{aligned} &\partial_\theta f|_{\theta=\pi/2} = 0, \quad \partial_\theta l|_{\theta=\pi/2} = 0, \quad \partial_\theta g|_{\theta=\pi/2} = 0, \\ &\partial_\theta \omega|_{\theta=\pi/2} = 0, \quad \partial_\theta \phi|_{\theta=\pi/2} = 0, \quad \partial_\theta V|_{\theta=\pi/2} = 0, \\ &\partial_\theta C|_{\theta=\pi/2} = 0. \end{aligned} \tag{15}$$

D. Conserved quantities

Charged boson stars are characterized by physical observables like mass M, angular momentum J, electric charge Q, respectively particle number N, as well as dipole moment μ. Here we discuss the interrelation of these quantities and how they are obtained. In a stationary asymptotically flat spacetime, the Komar expression provides a way to calculate global quantities directly associated with the Killing vectors. The mass and the angular momentum

$$M = 2\int_\Sigma R_{\mu\nu} n^\mu \xi^\nu dV, \qquad J = -\int_\Sigma R_{\mu\nu} n^\mu \eta^\nu dV, \tag{16}$$

are then calculated as an integral over a spacelike asymptotically flat hypersurface Σ bounded at spatial infinity. Here, $R_{\mu\nu}$ is the Ricci tensor, n^μ is a vector normal to Σ with $n^\mu n_\mu = -1$, and $dV = \sqrt{-\mathfrak{g}/f}\,dr d\theta d\varphi$ denotes the natural volume element. The metric (7) implies that $n^\mu = (\xi^\mu + \omega/r\eta^\mu)/\sqrt{f}$. Expressing the Ricci tensor in

terms of the energy-momentum tensor and employing the field equations, yields

$$M = \int (2T^t{}_t - T)\sqrt{-\mathfrak{g}} dr d\theta d\varphi,$$
$$J = -\int T^t{}_\varphi \sqrt{-\mathfrak{g}} dr d\theta d\varphi. \tag{17}$$

Local gauge symmetry gives rise to a conserved Noether current j^μ [Eq. (6)]. The associated electric charge Q can be obtained by integrating the projection of the current onto the future directed hypersurface normal n^μ and integrating over the whole space,

$$N = \int_\Sigma j_\mu n^\mu dV, \qquad Q = qN, \tag{18}$$

where N is considered as particle number of the star.

The integrand of the above equation is simply $-j^t\sqrt{-\mathfrak{g}}$. It is well known that for uncharged rotating boson stars $T^t{}_\varphi = mj^t$ and the angular momentum is quantized, assuming always values that are multiples of the particle number $J = mN$ [6]. The charged case is more involved. Here we show that the quantization relation valid for uncharged boson stars also holds for charged boson stars. We note that the integrand of the angular momentum can be written as

$$T^t{}_\varphi = mj^t + qA_\varphi j^t + F^{t\mu}F_{\varphi\mu}. \tag{19}$$

The third term can be rewritten as

$$F^{t\mu}F_{\varphi\mu} = F^{t\mu}\nabla_\varphi A_\mu - \nabla_\mu(F^{t\mu}A_\varphi) - qA_\varphi j^t, \tag{20}$$

where the Maxwell equation (5) has been used. The first term on the right-hand side is identically zero, the second one is a total divergence, which does not contribute to the integral ($A_\varphi = 0$ at infinity), and the third one cancels the second term in Eq. (19). Even though the integrands of J and N are different, after integration the quantization relation $J = mN$ still holds in the rotating charged case.

The global quantities M, J, Q, and furthermore the magnetic moment μ can be extracted from the asymptotic behavior of the metric and gauge field functions, as

$$M = \frac{1}{2}\lim_{r\to\infty} r^2\partial_r f, \qquad J = \frac{1}{2}\lim_{r\to\infty} r^2\omega,$$
$$Q = \frac{1}{2}\lim_{r\to\infty} r^2\partial_r V, \qquad \mu = \frac{1}{2}\lim_{r\to\infty} r^2\partial_r C. \tag{21}$$

III. NUMERICAL SOLUTIONS

The system comprises seven coupled nonlinear partial differential equations to be solved for four metric functions (f, l, g and ω) and three matter/gauge functions (ϕ, V and C). In order to solve this system numerically, we employ a two dimensional grid with a compactified radial coordinate $x = r/(r+1)$ where $x \in [0,1]$ covers the radial direction from zero to infinity, and $\theta \in [0, \pi/2]$ since all of the quantities have even parity with respect to reflections at the equatorial plane. The equations are then solved with the subroutines for elliptical PDEs of the FIDISOL package, with most grids containing 125×50 points and precision of 10^{-7}. For further discussion of the numerical method see [42] and, e.g., [43,44].

A. Domain of existence

The charged rotating boson stars are determined by the boson frequency ω_s, the gauge coupling parameter q, and the winding number m. We keep the winding number fixed, $m = 1$. For $q = 0$ the uncharged rotating boson stars are obtained. The charged rotating boson stars emerge from the uncharged rotating boson stars when the parameter q is increased. In the nonrotating case the range of the parameter q was discussed in [25,28]. In our study of rotating boson stars we found that solutions exist up to a maximal value of q. However, numerics fails when the maximal value is approached.

As for the uncharged rotating (and nonrotating) boson stars the range of ω_s is restricted to $\omega_{s,\min} < \omega_s < \omega_{s,\max}$, where $\omega_{s,\max} = m_b$. The minimal value $\omega_{s,\min}$ has to be determined numerically and depends on the gauge coupling parameter q. We observe that $\omega_{s,\min}$ increases with increasing values of q, leading to a restricted range of the frequency ω_s.

B. Observables

For convenience we will use the quantity $\phi_1 = \partial_r\phi|_{r=0}$ instead of ω_s as parameter. $\phi_1 = 0$ corresponds to $\omega_s = \omega_{s,\max}$.

The mass, angular momentum, charge, and magnetic moment as function of ϕ_1 are presented in Fig. 1 for some families of solutions. We observe that the mass and angular momentum increase with increasing charge for fixed value of ϕ_1. The maximum mass and angular momentum solution occurs for smaller values of ϕ_1 as the charge increases. As in the nonrotating case, the Coulomb repulsion between the star's components accounts to an equilibrium state at a higher mass value for the same value of ϕ_1 when compared to solutions with smaller gauge couplings.

In order to have some insight in the stability of these solutions, we refer to the diagrams in Fig. 2, where we show the mass as function of the particle number for fixed values of the gauge coupling parameter, together with the line representing N free bosons with mass m_b. The qualitative behavior is the same as described in [20,21]. The first branch comprehends the solutions with nontopological stability. It extends up to the maximal mass and maximal particle number, where it connects to a second branch which extends back to smaller masses and particle number. Along the

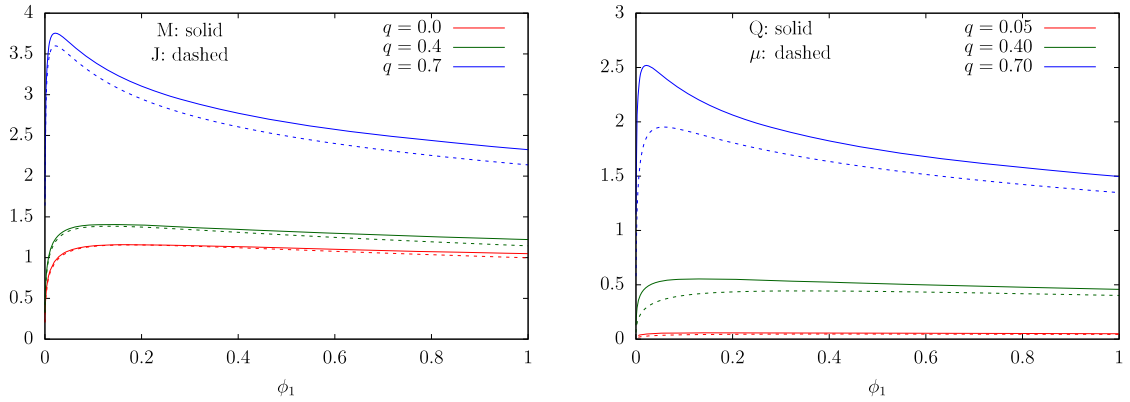

FIG. 1. Left: Mass (solid) and angular momentum (dashed) for rotating stars with $m = 1$, uncharged $q = 0$ and charged with $q = 0.4$ and $q = 0.7$. Right: Charge (solid) and magnetic moment (dashed) for three families of solutions with $m = 1$: $q = 0.05$, $q = 0.40$, $q = 0.70$.

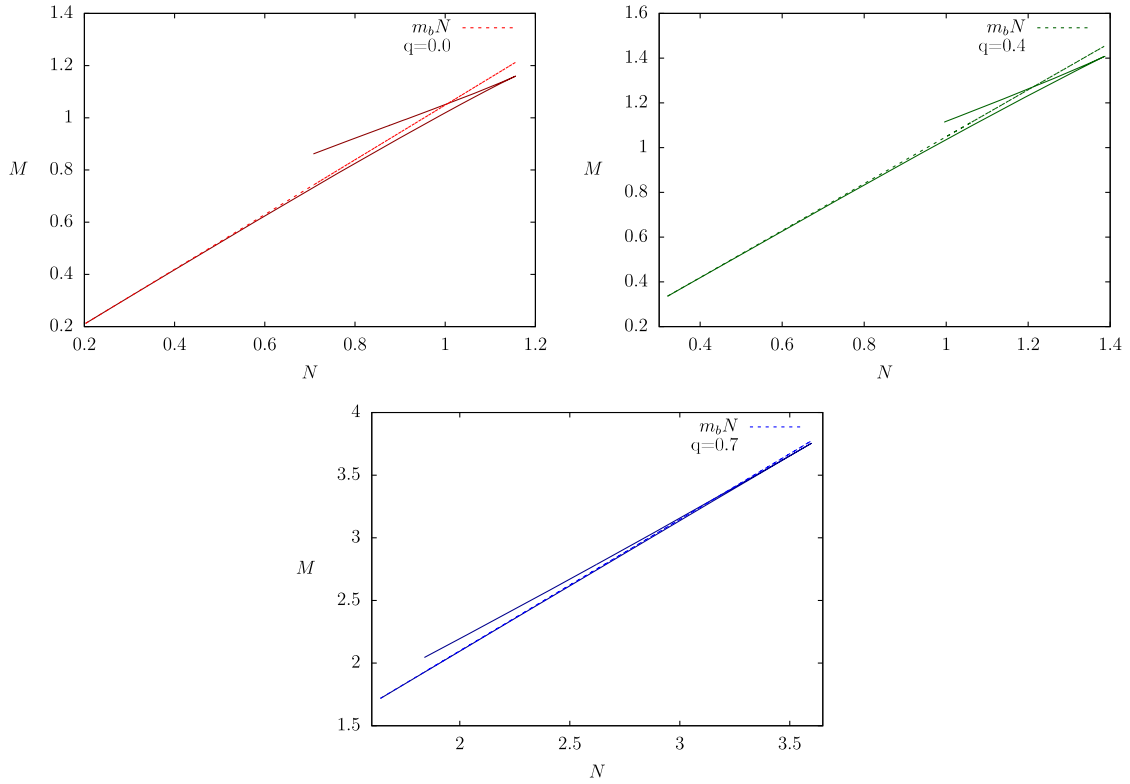

FIG. 2. Mass vs particle number for $m = 1$ and gauge coupling parameter $q = 0.0$, $q = 0.4$ and $q = 0.7$.

second branch the solutions possess larger mass at given particle number than the solutions on the first branch. Thus the solutions on the second branch are quantum mechanically unstable. Once the mass on the second branch exceeds the mass of free bosons (at given particle number) the boson stars are also classically unstable.

The new feature we observe is that the higher the value of the gauge coupling, the smaller is the difference between the mass of the boson star and the mass of free bosons with the same particle number.

The larger the gauge coupling, the larger the Coloumb repulsion of the particles of the star and the more its mass resembles that of a gas of separated particles.

C. Static ring

In a previous paper [24], we have shown that a class of spacetimes contains what we called the *static ring*: a ring of points in the equatorial plane, centered at the origin, where a particle initially at rest remains at rest. This class of spacetimes is assumed to be stationary, axisymmetric, and

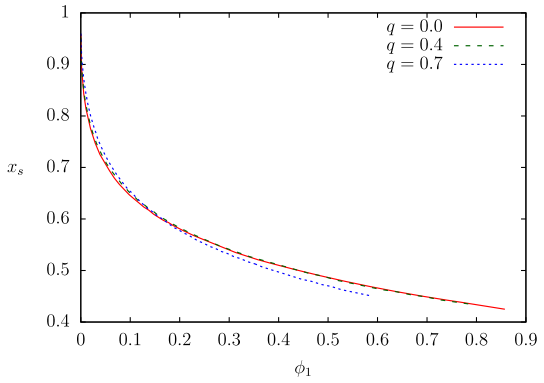

FIG. 3. Location of the static ring: the compactified coordinate x_s of the static ring is shown as function of the parameter ϕ_1.

circular. A necessary and sufficient condition for the existence of such ring is that the g_{tt} component of the metric possesses a local maximum at a point where it is negative, i.e., not in an ergoregion. Boson stars and highly compact objects surrounded by a massive bosonic cloud are the most prominent sources of this class of spacetimes and the rotating charged boson star is no different.

The radius of the static ring for three different families of solutions is illustrated in Fig. 3. All of the solutions, for every value of the gauge coupling parameter and ϕ_1, the function g_{tt} shows qualitatively the same behavior, containing a local maximum in the equatorial plane. Figure 3 shows the compactified coordinate of the static rings as function of the parameter ϕ_1 for fixed gauge coupling parameter q. The curves terminate at a specific point where the static ring enters the ergoregion, in which no timelike particle could stay at rest.

As the gauge coupling increases, the radius of the static ring decreases slightly and the curves terminate at smaller values of ϕ_1. Hence the radius of the static ring does not depend strongly on the gauge coupling parameter.

The more distinctive change of behavior as the coupling increases is the terminating point, which happens for smaller values of ϕ_1. Since the angular momentum J increases due to a more prominent gauge field, A_μ, ergoregions are prone to appear earlier in the parameter space, even though all sets are described by the same rotation number.

IV. COMOVING OBSERVER

In order to have a clear realization of the energy density and pressures separately, we adopt comoving coordinates, i.e., for which the energy momentum tensor is diagonal. These quantities are then the eigenvalues that satisfy

$$T^{\mu}{}_{\nu}\hat{e}^{\nu}{}_{(a)} = \lambda_{(a)}\hat{e}^{\mu}{}_{(a)}, \tag{22}$$

where $\hat{e}^{\mu}_{a}$ are the energy momentum tensor's eigenvectors.

The eigenvalues and eigenvectors found through the equation above are rather long for the system we are describing. Nevertheless, for any circular, stationary and axisymmetric spacetime, we can hide the extensive expressions in notation by splitting the energy momentum tensor as

$$T_{\mu\nu} = \mathcal{T}^{(1)}_{\mu\nu} + \mathcal{T}^{(2)}_{\mu\nu}, \tag{23}$$

with

$$\mathcal{T}^{(1)}_{\mu\nu} = \begin{pmatrix} T_{tt} & 0 & 0 & T_{t\varphi} \\ 0 & 0 & 0 & 0 \\ 0 & 0 & 0 & 0 \\ T_{t\varphi} & 0 & 0 & T_{\varphi\varphi} \end{pmatrix}, \quad \mathcal{T}^{(2)}_{\mu\nu} = \begin{pmatrix} 0 & 0 & 0 & 0 \\ 0 & T_{rr} & T_{r\theta} & 0 \\ 0 & T_{r\theta} & T_{\theta\theta} & 0 \\ 0 & 0 & 0 & 0 \end{pmatrix}.$$

Then the eigenvalues of $T_{\mu\nu}$ are given by

$$\lambda_{i\pm} = \frac{1}{2}\left[\pm\sqrt{2\mathcal{T}^{\mu\nu}\mathcal{T}_{\mu\nu} - \mathcal{T}^2} + \mathcal{T}\right]_{(i)}, \tag{24}$$

where $\mathcal{T}^{(i)} = g^{\mu\nu}\mathcal{T}^{(i)}_{\mu\nu}$.

A. Nonrotating boson stars

In the interest of comparison, we shall consider the spherically symmetric charged boson stars, again employing isotropic coordinates. In this case $\omega = 0$, $g = 1$, and $C = 0$ and f, l, ϕ, and V are functions of r only. The energy density and pressures then read

$$\begin{aligned} \rho &= \frac{f}{l}\phi'^2 + \frac{V'^2}{2l} + \frac{\phi^2}{f}(Vq + \omega_s)^2 + U(|\Phi|), \\ p_r &= \rho - \frac{V'^2}{l} - 2U(|\Phi|), \\ p_\perp &= \rho - 2\frac{f}{l}\phi'^2 - 2U(|\Phi|). \end{aligned} \tag{25}$$

The uncharged case is obtained simply by setting $q = 0$ and $V = 0$.

B. Rotating boson stars

The rotating case is of course more involved. Let us first consider the uncharged rotating boson stars. The hydrodynamic quantities obtained via Eq. (24) are [45]

$$\rho = \frac{f}{lgr^2}[r^2(\partial_r\phi)^2 + (\partial_\theta\phi)^2] + \frac{|f^2m^2 - l\sin^2\theta(m\omega + \omega_s r)^2|}{flr^2\sin^2\theta}\phi^2 + U(|\Phi|),$$
$$p_r = \frac{f}{lgr^2}[r^2(\partial_r\phi)^2 + (\partial_\theta\phi)^2] - \frac{f^2m^2 - l\sin^2\theta(m\omega + \omega_s r)^2}{flr^2\sin^2\theta}\phi^2 - U(|\Phi|),$$
$$p_\theta = p_r - 2\frac{f}{lgr^2}[r^2(\partial_r\phi)^2 + (\partial_\theta\phi)^2],$$
$$p_\varphi = \rho - 2\frac{f}{lgr^2}[r^2(\partial_r\phi)^2 + (\partial_\theta\phi)^2] - 2U(|\Phi|). \quad (26)$$

There are two new features induced by rotation worth of notice. First, the system becomes what we decide to call *completely anisotropic*, meaning $p_r \neq p_\theta \neq p_\varphi$. Second, the energy density and axial pressure show a cusp due to the absolute value term, whose argument changes sign at a point where

$$-f^2m^2 + lr^2\sin^2\theta\left(\omega_s + m\frac{\omega}{r}\right)^2 = 0 \Leftrightarrow m^2 g_{tt} - 2m\omega_s g_{t\varphi} + \omega_s^2 g_{\varphi\varphi} = 0. \quad (27)$$

It is straightforward to understand that this point must occur for all solutions: at the origin the only surviving term is g_{tt} (which is negative), while at large distances the dominant term is $g_{\varphi\varphi}$ (which is always positive). The structure of Eq. (27) tempts us to define the parameter vector $w^\mu = (m, 0, 0, -\omega_s)$ that is timelike at the center of the star, becomes null at the cusp and finally turns spacelike from that point all the way to infinity. We note that the Killing vector field $K' = w^\mu\partial_\mu$ possesses the property $K'\Phi = 0$. At the cusp, this property translates to $j^\mu j_\mu = 0$.

The change of sign has also consequences for the eigenvectors. In the region where w^μ is timelike, the timelike eigenvector can be expressed as $\hat{e}^\mu{}_{(1-)} = w^\mu/\sqrt{-w^\mu w_\mu}$, whereas in the region where w^μ is spacelike, $\hat{e}^\mu{}_{(1-)} = v^\mu/\sqrt{-v^\mu v_\mu}$, where v^μ is orthogonal to w^μ, i.e., $v^\mu w_\mu = 0$.

Let us consider an observer in the comoving frame and identify her four velocity with the timelike eigenvector $U^\mu = (U^t, 0, 0, U^\varphi) = \hat{e}^\mu{}_{(1-)}$. The energy $E = -g_{t\mu}U^\mu$ and the angular momentum $L = g_{\varphi\mu}U^\mu$ both will diverge, if she approaches the cusp. Hence we conclude, that the cusp corresponds to a pathology of the comoving frame. An observer approaching the cusp would need an infinite amount of energy in order to stay in the comoving frame. Moreover, the cusp surface envelops a volume where the four current is spacelike and $j_\mu\hat{e}^\mu{}_{(1-)} = 0$, i.e., the observer measures zero particle number density.

Let us next consider the charged rotating boson stars. The equations describing the hydrodynamic quantities are lengthy and cumbersome, therefore we do not show them fully here but express them around the center and axis of rotation. Keeping only the leading order contribution for each field, we have that at $r \approx 0$

$$f \approx f_c, \quad l \approx l_c, \quad g \approx 1, \quad \omega \approx \omega_c r, \quad \phi \approx \phi_{cm} r^m \sin^m\theta, \quad V \approx V_c, \quad C \approx C_{c2} r^2 \sin^2\theta, \quad (28)$$

while at $\theta \approx 0$

$$f \approx f_0(r), \quad l \approx l_0(r), \quad g \approx 1, \quad \omega \approx \omega_0(r), \quad \phi \approx \phi_m(r)\theta^m, \quad V \approx V_0(r), \quad C \approx C_2(r)\theta^2. \quad (29)$$

The energy density and pressures at the center then yield

$$\rho = 2\frac{\phi_{c1}^2 f_c}{l_c} + 2\left(\frac{C_{c2}f_c}{l_c}\right)^2, \quad p_r = 2\left(\frac{C_{c2}f_c}{l_c}\right)^2, \quad p_\theta = -\rho, \quad p_\varphi = p_r, \quad (30)$$

and at $\theta = 0$,

$$\rho = 2\frac{\phi_1^2(r)f_0(r)}{l_0(r)r^2} + \frac{V_0'^2(r)}{2l_0(r)} + 2\left(\frac{C_2(r)f_0(r)}{l_0(r)r^2}\right)^2, \quad p_r = \frac{V_0'^2(r)}{2l_0(r)} + 2\left(\frac{C_2(r)f_0(r)}{l_0(r)r^2}\right)^2, \quad p_\theta = -\rho, \quad p_\varphi = p_r. \quad (31)$$

The energy density of a rotating boson star with $m = 1$ is then nonzero at the origin, even when uncharged, although the scalar field vanishes at that point. At higher rotation numbers, the charged boson star maintains nonzero density at the symmetry axis, as opposed to the uncharged rotating star. We stress the similar behavior for the trace of the energy momentum tensor T^μ_μ, which is always negative for $\theta = 0$ for $m = 1$, but zero on that axis for $m > 1$.

We show in Fig. 4 the energy density in the equatorial plane for the uncharged rotating boson stars (left) and the charged rotating boson stars with gauge coupling parameter $q = 0.7$ (right) for several values of ϕ_1 and $m = 1$. In the uncharged case the energy density possesses a local maximum at the center, a local minimum corresponding to the cusp, and a maximum in the equatorial plane. This is in contrast to the charged case when no cusp is present. Thus for the charged rotating boson stars the energy density possesses a local minimum at the center and a maximum in the equatorial plane.

With increasing values of the parameter ϕ_1 the magnitudes of the minima and the maxima increase and the locations of the maxima and the cusp move closer to the center. Note that, in both cases, the central density can be

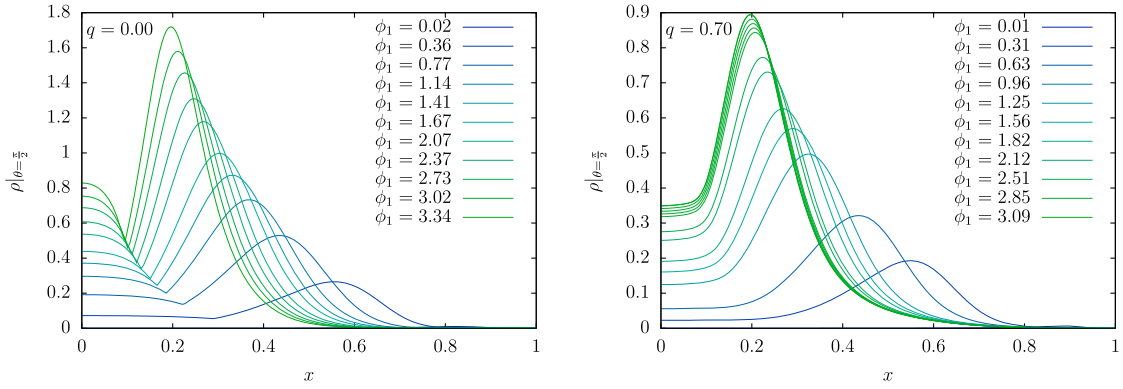

FIG. 4. Profile of the energy density on the equatorial plane for boson stars with rotation number $m = 1$. Left: Uncharged rotating boson star. Right: Charged rotating boson star.

significantly high, despite the vanishing scalar field on the symmetry axis.

In Fig. 5 we illustrate how the maximum of the energy density and anisotropic pressures vary with respect to the maximum of the scalar field for solutions with different values of the gauge coupling parameter, as well as the minimum of the tangential pressures and trace of the energy momentum tensor. The energy density and radial pressure are everywhere positive and their global minimum is therefore zero, similarly the trace of the energy momentum tensor has its maximum at zero for being everywhere negative definite. The uncharged rotating solution, although already completely anisotropic, features for every solution the same maximum value for all three pressures. With increasing gauge coupling the maxima and minima of all hydrodynamic quantities become smaller, but the curves giving the maximum value of the pressures start to separate from each other. For $q = 0.4$ we notice that the maximum value of p_φ is always bigger than those of p_r and p_θ which lie on the same curve, and for $q = 0.7$ we notice the p_θ curve appearing below the maximum radial pressure one. We stress that we need to go to very large couplings, near the limiting q_{crit}, to be able to observe such small deviations.

For completeness, we show in Fig. 6 how the maximum values of the pressures vary with the rotation number m. The domain of existence of boson stars with $m = 2$ is more restricted as compared to the case with $m = 1$. The density grows much more rapidly with increasing ϕ_2, and the maximum of the scalar field takes smaller values when compared with $m = 1$. As the rotation number assumes larger values, the dynamical properties of the boson star tend to be more and more dominated by its kinetic terms in the energy momentum tensor. Furthermore, increasing m has an analogous effect on the maximum of pressures as does an increasing charge, i.e., they decrease in value and the curves become distinct. No difference was noted for the energy density or minimum of such quantities.

In the three figures that follow, we present three different rotating boson stars for comparison. The first boson star is

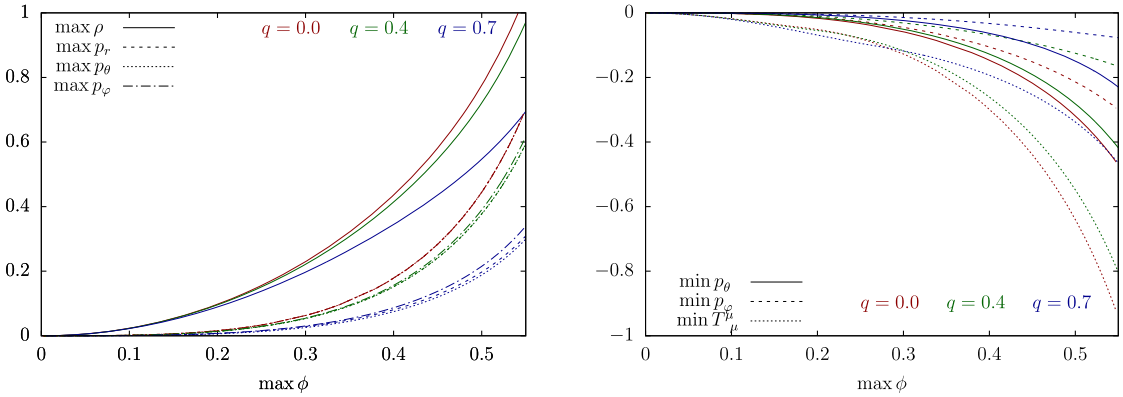

FIG. 5. Left: Maximum value of the hydrodynamic quantities for uncharged and charged rotating boson stars as function of the maximum value of the scalar field for each solution. The higher the coupling value, the smaller these quantities become, but the lines tend to spread away enhancing the complete anisotropy. Right: Minimum value of the anisotropic tangential pressures and trace of the energy momentum tensor as functions of the maximum value of the field. The minimum value of the energy density and radial pressure is zero and therefore not depicted. Again here, by increasing the charge, the minimum value is mitigated.

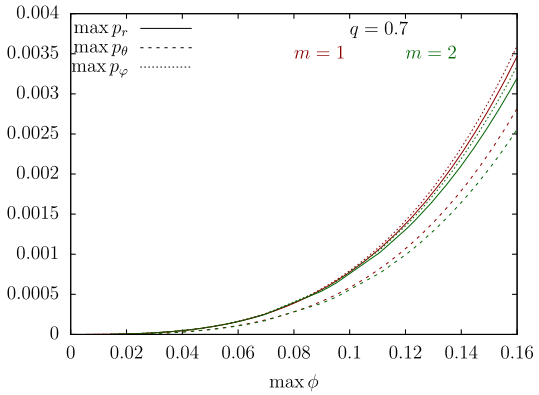

FIG. 6. Maximum of pressures for rotating charged boson stars with rotation numbers $m = 1$ and $m = 2$ as functions of the maximum of the scalar field. Rotation has a similar effect on these quantities as does the charge, decreasing their maximum value and slightly pushing these curves further apart.

uncharged, $q = 0$ and has rotation number $m = 1$. The second and third both have the same coupling charge, $q = 0.7$, but the latter possesses rotation number $m = 2$. Each of these solutions corresponds to the one with the maximum mass for fixed m and q. In these images and the others that will appear later, $z = \bar{r}\cos\theta$ is parallel to the rotation axis and $x = \bar{r}\sin\theta$ to the equatorial plane, where $\bar{r} = r/(r+1)$ is the compactified radial coordinate.

The energy density and radial pressure are depicted in Fig. 7. The comoving observer measures the energy density to be a lot higher off center, being negligible at the core for the $m = 2$ star, as according to Eq. (30) only $\partial_r^2 C$ contributes at this point, and its value is fairly low. For the uncharged case, we can entertain the kink in the energy density discussed above, as its value drops harshly to a local minimum and then grows back up to the global maximum with increasing r, and we see a thin dark line that spans through all the polar coordinate. Furthermore, in this same case the radial pressure is zero at the origin and negligible outside the neighborhood of its maximum value. The faster rotating star, as seen by the comoving observer, has a thinner density bag which sits further away from the origin as one would expect. The profile of the radial pressure is quite similar, but we notice how the bag is somewhat spread to smaller values of θ.

In Fig. 8, the two tangential pressures are illustrated, and we are able to acknowledge how distinct they are. For $m = 1$, the polar pressure is highly negative near the center while the axial one is mildly positive for the charged case and zero for $q = 0$. In all three stars, in the panel for p_φ, there is an empty, pressureless shell which encompasses a region where the sign of the pressure switches. At higher distances from the center, the axial pressure becomes once again positive, and we notice that all pressures have their maximum value near the point of highest energy density. As before, we notice how these quantities distribute themselves over a wider range in the polar coordinate for $m = 2$, while getting narrower in r.

The scalar field, which sources the electromagnetic field is drawn in Fig. 9 together with the trace of the energy momentum tensor. The ϕ^2 profile has the shape of a torus, as could be anticipated by the boundary conditions. The trace of the energy momentum tensor, which is zero for the electromagnetic field, takes now negative values.

V. ELECTROMAGNETIC FIELD

The two invariants of the electromagnetic field are seen in Fig. 10, where ${}^*F_{\mu\nu} = \frac{1}{2}\epsilon_{\mu\nu\sigma\lambda}F^{\sigma\lambda}$ is the dual of the field and $\epsilon_{\mu\nu\sigma\lambda}$ is the Levi-Civita tensor. The invariants for a Kerr-Newman black hole which possesses the same mass, charge and angular momentum as the analyzed boson star with $m = 1$, is also given at the bottom, where the black disc represents its event horizon and we show only the contracted fields in the exterior region. The general behavior is drastically different. Both invariants extend to much larger regions in comparison with the Kerr-Newman black hole, since their charge concentrates off center and the main resemblance is the orthogonality between the fields on the equatorial plane, which could be anticipated from the boundary conditions we established. Rotating charged boson stars feature a region of strong magnetic dominance, which is lacking in rotating charged black holes.

As a means to visualize the electric and magnetic field individually, we need to adopt a reference frame since those are not invariant quantities. Therefore, we choose the local inertial frame of a zero angular momentum observer (ZAMO), the only one capable of inertially reaching the center of the star, see [22–24]. The fields are then given by

$$E_\mu = F_{\mu\nu}\chi^\nu; \qquad B_\mu = -\frac{1}{2}\epsilon_{\mu\nu\sigma\gamma}F^{\nu\sigma}\chi^\gamma, \tag{32}$$

where χ^μ is the four-velocity of the ZAMO, which reads in general form (in a stationary, axisymmetric spacetime),

$$\chi^\mu = \sqrt{-g^{tt}}\left(1, 0, 0, \frac{g^{t\varphi}}{g^{tt}}\right), \tag{33}$$

and one should note that, indeed, $\chi_\varphi = L = 0$.

These fields, as seen by the ZAMO, are given in Fig. 11 for the two previously illustrated charged boson stars. The electric field is stronger in a thin shell that encompasses the region where the scalar field is maximum, in the *exterior* region. In the *interior* region, i.e., for smaller radii than the position of the maximum of the scalar field, the electric field is very weak on the equatorial plane. The magnetic field is fairly strong and homogeneous in this region. The qualitative behavior of the fields is very similar indeed to that of a thick circular loop.

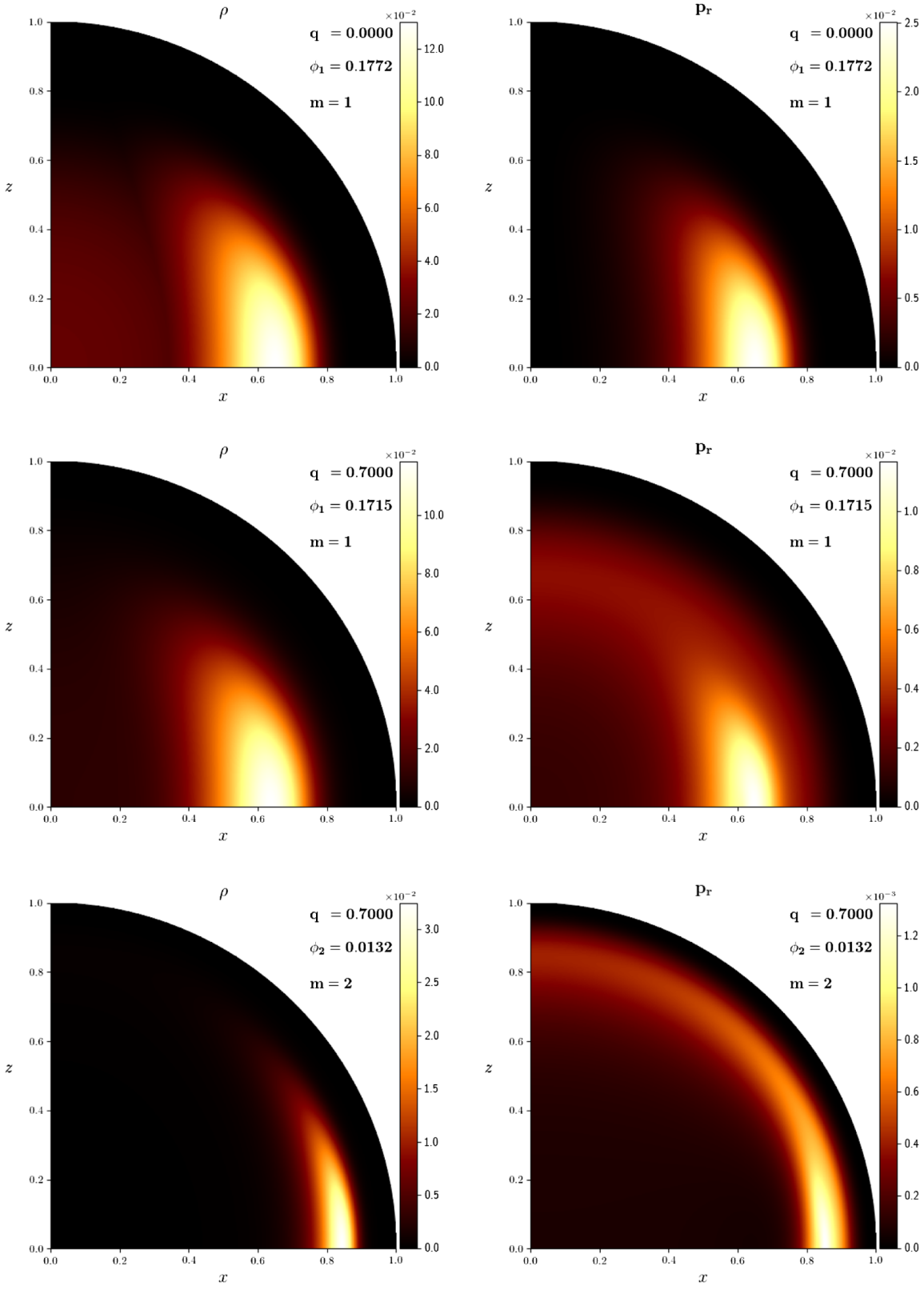

FIG. 7. Energy density and radial pressure as seen by an observer comoving with the fluid of a rotating charged boson star for different charges and rotation numbers.

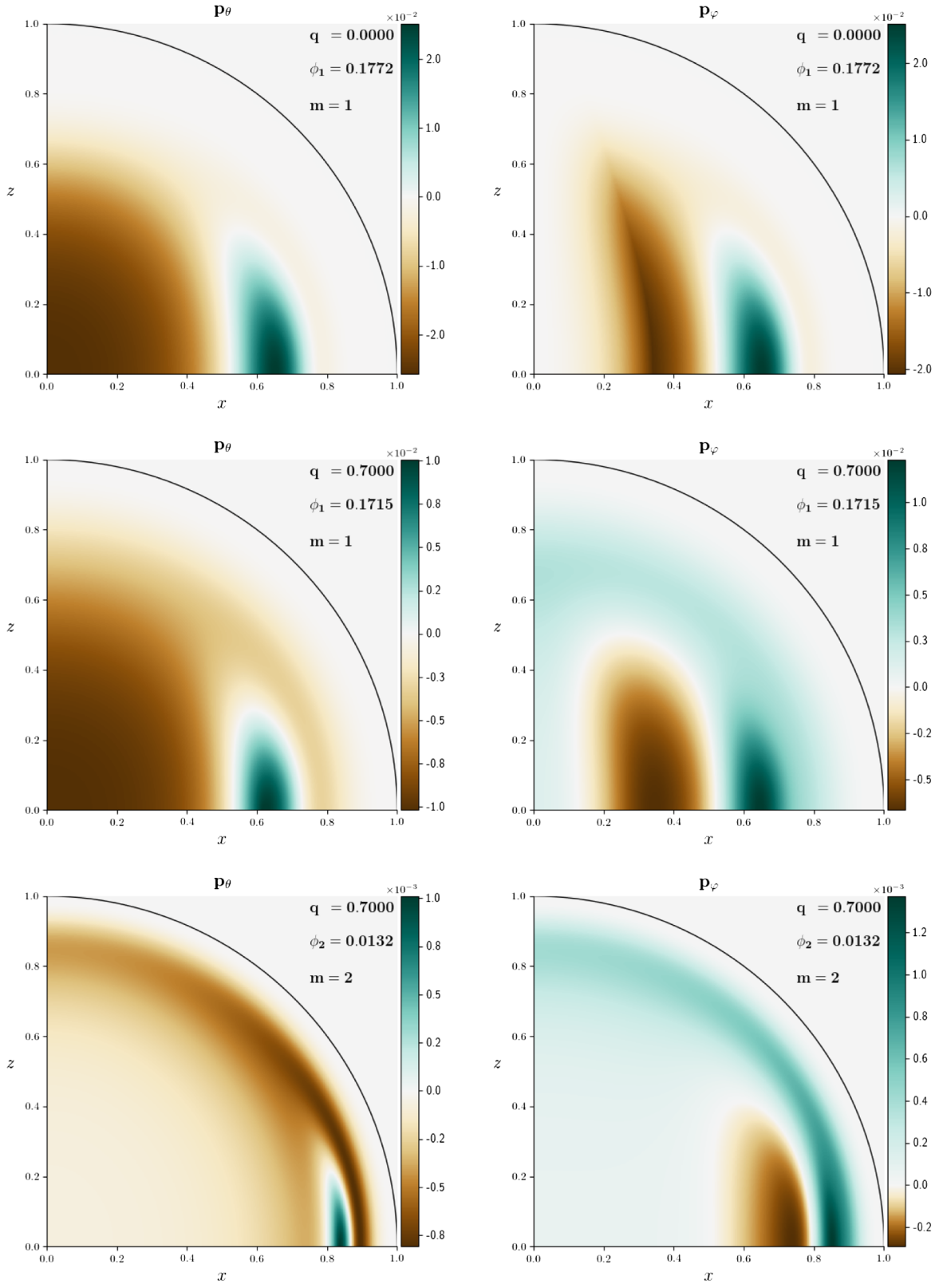

FIG. 8. Polar and axial pressures for the same stars as in 7, as measured by the comoving observer.

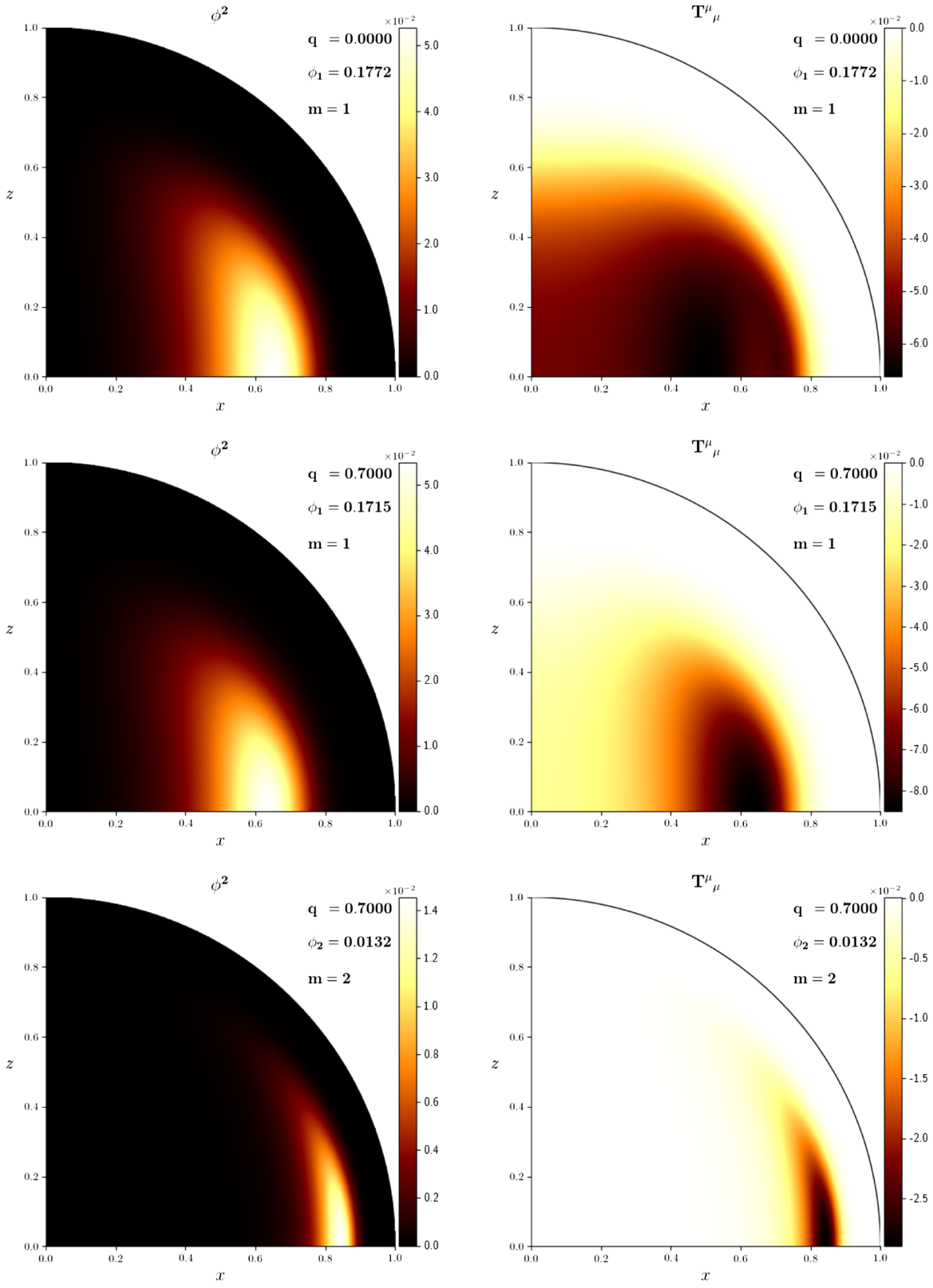

FIG. 9. The square of the scalar field (photon's mass) and the trace of the energy momentum tensor for the same stars as in 7 and 8.

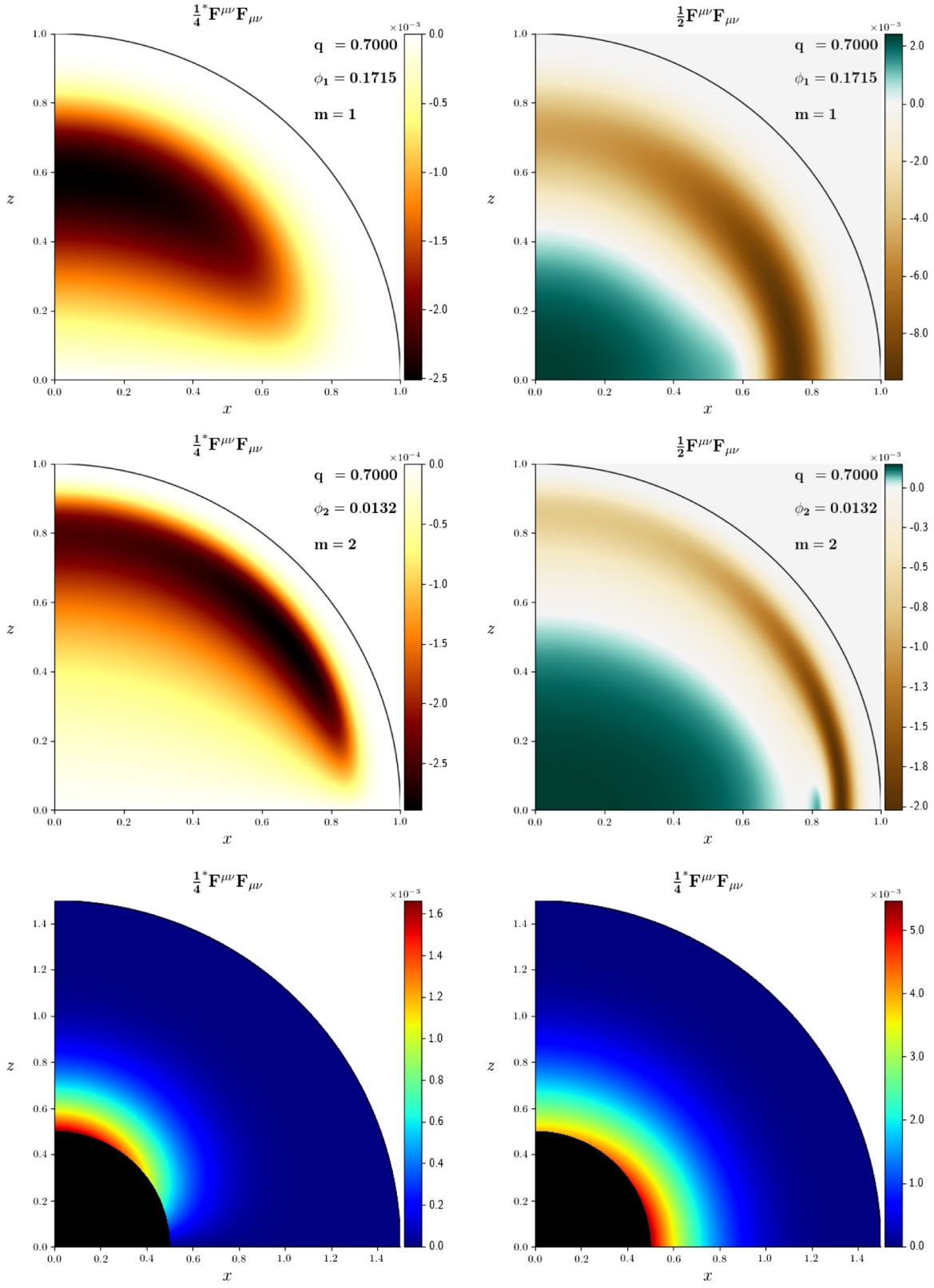

FIG. 10. Invariants of the electromagnetic fields for the two charged boson stars shown in the previous figures and a Kerr-Newman black hole (bottom) with the same mass, charge and spin as the star on the top panel. For the black hole, only the exterior values are shown. The black disc covers the inner horizon region.

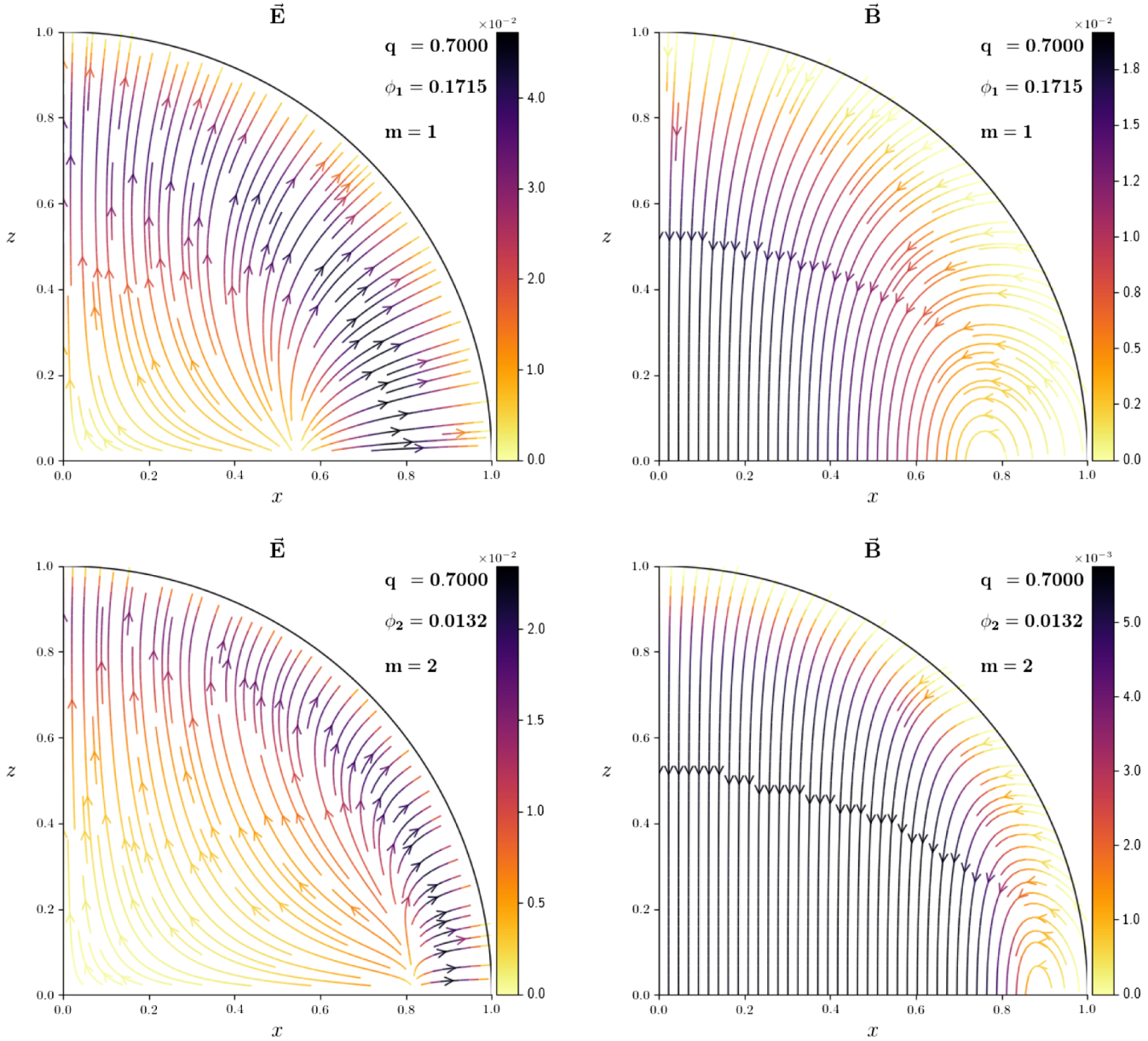

FIG. 11. Electric and magnetic field as measured by the ZAMO.

VI. CONCLUSION

In the present work we revisited boson stars in their most general form, possessing angular momentum and charge. Treating the fields as fluids in a comoving local frame, the hydrodynamic quantities were obtained in an unambiguous form. The yielded relationships entertain the completely anisotropic character of rotating boson stars, charged or not, that contain three different kinds of pressures associated each with a spacelike tetrad basis component. We showed that the uncharged rotating boson star has, increasingly with its central density, a point where the variation of its energy density diverges, due to an absolute value term in its expression, which is also present in its relation for the axial pressure. Furthermore, these quantities are not zero at the core, as opposed to the scalar field. As the charge coupling increases, the curves describing the maximum and minimum of each of the hydrodynamic variables diverge from each other. Unlike most anisotropic stars constructed in an *ad hoc* manner, the different tangential pressures of a boson star assume at points negative values.

Measurable entities, such as mass, angular momentum, total charge, and magnetic moment were also drawn for different configuration sets. As one increases the charge coupling, all of these observables take higher values for the same value of the leading order term of the scalar field at the origin. Thus, the onset of ergoregions occurs earlier for stars with higher charge coupling q, terminating the existence of a static ring for timelike particles.

The invariants of the electromagnetic field were shown for solutions with different rotation quantum number m, in comparison to a Kerr-Newman black hole with same mass, angular momentum and charge as one of the depicted solutions. Even though their order of magnitude is the same, the distribution is entirely different thanks to the nontrivial topology of the scalar field which carries the charge. As seen by a ZAMO, the rotating charged boson star produces a fairly homogeneous magnetic field in a neighborhood of the equatorial plane in a region between the center of the star and the densest part of the torus.

ACKNOWLEDGMENTS

We would like to acknowledge support by the DFG Research Training Group 1620 *Models of Gravity* as well as by FP7, Marie Curie Actions, People, International Research Staff Exchange Scheme (IRSES-606096), COST Action CA16104 GWverse.

[1] D. J. Kaup, Phys. Rev. **172**, 1331 (1968).
[2] D. A. Feinblum and W. A. McKinley, Phys. Rev. **168**, 1445 (1968).
[3] R. Ruffini and S. Bonazzola, Phys. Rev. **187**, 1767 (1969).
[4] P. Jetzer and J. J. van der Bij, Phys. Lett. B **227**, 341 (1989).
[5] S. Yoshida and Y. Eriguchi, Phys. Rev. D **56**, 762 (1997).
[6] E. W. Mielke and F. E. Schunck, in *Gravity, Particles, and Space-Time*, edited by P. Pronin and G. Sardanashvili (World Scientific, Singapore, 1996), pp. 391–420.
[7] Y. Kobayashi, M. Kasai, and T. Futamase, Phys. Rev. D **50**, 7721 (1994).
[8] M. Colpi, S. L. Shapiro, and I. Wasserman, Phys. Rev. Lett. **57**, 2485 (1986).
[9] R. Friedberg, T. D. Lee, and Y. Pang, Phys. Rev. D **35**, 3658 (1987).
[10] W. Deppert and E. W. Mielke, Phys. Rev. D **20**, 1303 (1979).
[11] S. R. Coleman, Nucl. Phys. **B262**, 263 (1985); **B269**, 744(E) (1986).
[12] J. Barranco and A. Bernal, Phys. Rev. D **83**, 043525 (2011).
[13] F. D. Ryan, Phys. Rev. D **55**, 6081 (1997).
[14] F. E. Schunck and E. W. Mielke, Phys. Lett. A **249**, 389 (1998).
[15] F. E. Schunck and E. W. Mielke, Gen. Relativ. Gravit. **31**, 787 (1999).
[16] E. W. Mielke and F. E. Schunck, Nucl. Phys. **B564**, 185 (2000).
[17] B. Kleihaus, J. Kunz, and M. List, Phys. Rev. D **72**, 064002 (2005).
[18] B. Kleihaus, J. Kunz, M. List, and I. Schaffer, Phys. Rev. D **77**, 064025 (2008).
[19] B. Hartmann, B. Kleihaus, J. Kunz, and M. List, Phys. Rev. D **82**, 084022 (2010).
[20] B. Kleihaus, J. Kunz, and S. Schneider, Phys. Rev. D **85**, 024045 (2012).
[21] L. G. Collodel, B. Kleihaus, and J. Kunz, Phys. Rev. D **96**, 084066 (2017).
[22] P. Grandclément, C. Som, and E. Gourgoulhon, Phys. Rev. D **90**, 024068 (2014).
[23] M. Grould, Z. Meliani, F. H. Vincent, P. Grandclément, and E. Gourgoulhon, Classical Quantum Gravity **34**, 215007 (2017).
[24] L. G. Collodel, B. Kleihaus, and J. Kunz, Phys. Rev. Lett. **120**, 201103 (2018).
[25] P. Jetzer, Phys. Lett. B **231**, 433 (1989).
[26] P. Jetzer, CERN Report No. CERN-TH-5681/90, 1990.
[27] P. Jetzer, P. Liljenberg, and B. S. Skagerstam, Astropart. Phys. **1**, 429 (1993).
[28] D. Pugliese, H. Quevedo, J. A. Rueda H., and R. Ruffini, Phys. Rev. D **88**, 024053 (2013).
[29] N. Kan and K. Shiraishi, Eur. Phys. J. C **78**, 257 (2018).
[30] B. Kleihaus, J. Kunz, C. Lammerzahl, and M. List, Phys. Lett. B **675**, 102 (2009).
[31] B. Kleihaus, J. Kunz, C. Lammerzahl, and M. List, Phys. Rev. D **82**, 104050 (2010).
[32] S. Kumar, U. Kulshreshtha, and D. Shankar Kulshreshtha, Classical Quantum Gravity **31**, 167001 (2014).
[33] S. Kumar, U. Kulshreshtha, and D. S. Kulshreshtha, Phys. Rev. D **93**, 101501 (2016).
[34] S. Kumar, U. Kulshreshtha, D. S. Kulshreshtha, S. Kahlen, and J. Kunz, Phys. Lett. B **772**, 615 (2017).
[35] E. Radu and M. S. Volkov, Phys. Rep. **468**, 101 (2008).
[36] Y. Brihaye, T. Caebergs, and T. Delsate, arXiv:0907.0913.
[37] O. Kichakova, J. Kunz, and E. Radu, Phys. Lett. B **728**, 328 (2014).
[38] J. F. M. Delgado, C. A. R. Herdeiro, E. Radu, and H. Runarsson, Phys. Lett. B **761**, 234 (2016).
[39] E. W. Mielke and R. Scherzer, Phys. Rev. D **24**, 2111 (1981).
[40] M. S. Volkov and E. Wohnert, Phys. Rev. D **66**, 085003 (2002).
[41] L. A. Urena-Lopez, Classical Quantum Gravity **19**, 2617 (2002).
[42] W. Schönauer and R. Weiß, J. Comput. Appl. Math. **27**, 279 (1989); M. Schauder, R. Weiß, and W. Schönauer, The CADSOL Program Package, Interner Bericht No. 46/92, Universität Karlsruhe, 1992.
[43] B. Kleihaus and J. Kunz, Phys. Rev. D **57**, 834 (1998).
[44] B. Kleihaus, J. Kunz, and E. Radu, J. High Energy Phys. 01 (2015) 117.
[45] In [21] we have overlooked that a term should actually be an absolute value and reported incorrect expressions.